ISSUE: April 2025

Designing An Open-Source Power Inverter (Part 25): Boost Or Buck For Converters That Increase Voltage?

by Dennis Feucht, Innovatia Laboratories, Cayo, Belize

This long and winding articles series on the Volksinverter,[1-24] a battery-powered inverter whose design is open source for the benefit of engineers, technicians and other qualified individuals, is now coming to its end. The series started about four years ago with a basic structure for the inverter mapped out, specifications for the overall inverter and each of its stages, and prototype designs built for each of the inverter's two power conversion stages (Fig. 1). From that start, we have worked through the theory and procedures for designing each of these stages, covering the design of control and power circuitry, magnetics and filter design.

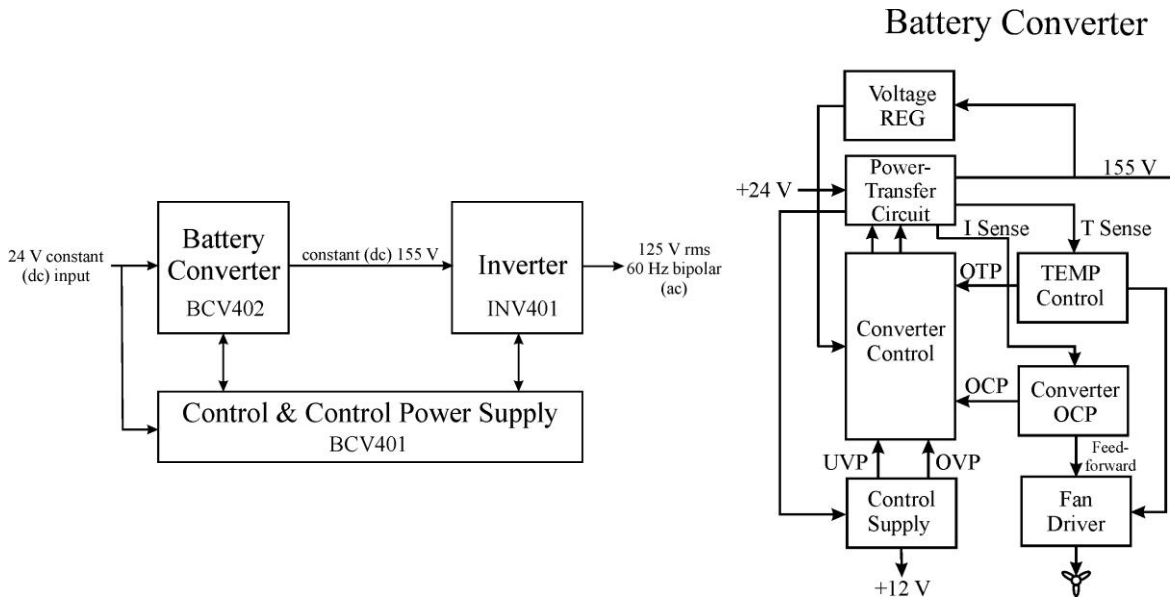

Fig. 1. The Volksinverter's system block diagram (left) and the BCV402 battery converter stage block diagram (right).

A key element of this process has been evaluating different design alternatives along the way, both for the purposes of optimizing this particular design to the given specifications and also to make it broadly applicable to other inverter project requirements that the reader may encounter, and even other converter types. For example with respect to design alternatives, much discussion was devoted to the selection of the battery converter's power transfer circuit.

In part 3 we compared the push-pull (PP), boost push-pull (CA-BPP) and SEPIC topologies, as possible options. Then we considered the differential BPP in part 13 and the bridge-switched common-passive or buck (CP-BRG) in part 14 as further options. To this point we've stuck with the CA-PP as best (if barely so) for our particular set of design specifications.

However, in retrospect, was the Volksinverter choice of the CA (boost) transfer circuit optimal in view of residential inverter convergence to a CP (buck) configuration instead? If we look back at the previous comparisons of the buck and boost circuits, we'll see that there were some differences between these circuits that complicate the comparisons. The CP-PP circuit we are about to examine is slightly different from the PP and CP-BRG buck circuits previously examined, and is more structurally similar to the CA-PP to allow a more direct comparison of buck versus boost. In this analysis, we'll work through the design equations that will influence the design of the transformer in each circuit, compare the current form factors of the transformer and power switches in each case as these reflect losses, and also consider differences in waveforms, and design power ratios.

CP-PP Versus Boost CA-PP—Different Magnetics

Commercial battery-inverter design for the residential market has a two-stage scheme of a voltage-increasing converter stage followed by an inverter that generates the bipolar output waveform. The respectable commercial power-transfer circuit has converged to the topology shown in Fig. 2 (top diagram): a push-pull common-passive (CP or buck) PWM-switch configuration.

With this topology, the transformer is required to achieve the higher output voltage, which for the Volksinverter has a nominal design value of Vc = 160 V with an input-port voltage nominally rated at Vg = 24 V and an operational range from 20 V to 30 V. The nominal voltage gain is Vo /Vg = 6.67, a substantial increase in voltage.

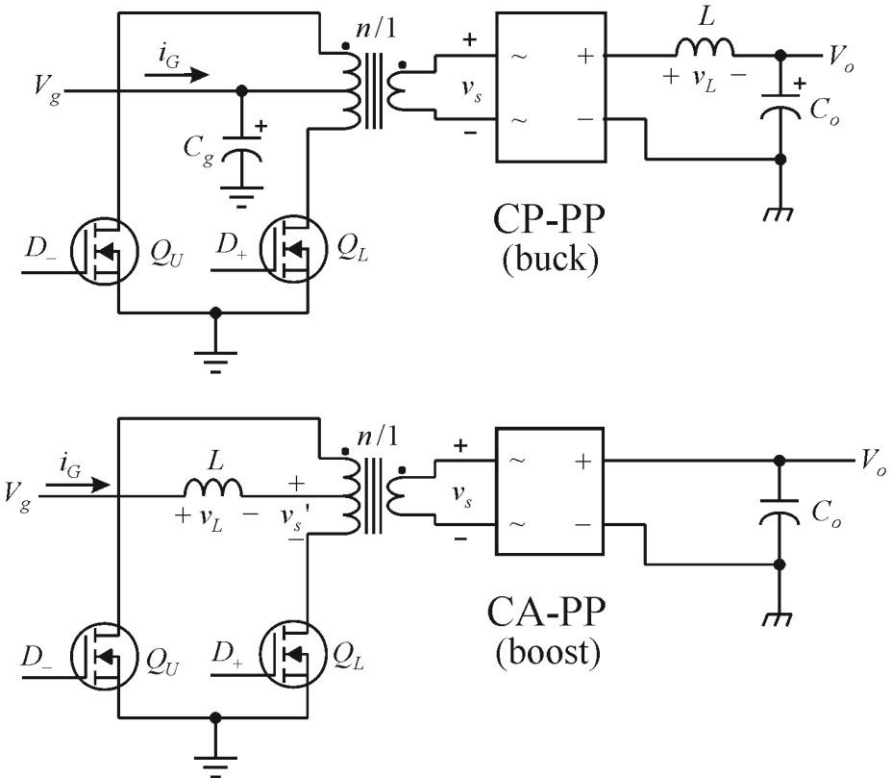

Fig. 2. Typical commercial (residential) converter transfer circuit with a push-pull primary circuit and CP (buck) configuration with the inductor L in the secondary circuit (top) versus the Volksinverter CA (boost) push-pull circuit (bottom).

The CP circuit applies input voltage V_g to primary windings on the input side. The on-time primary voltage $V_p = V_g$. The CA circuit connects (through the rectifier) the secondary winding to the output so that $V_s = V_o$. The inverse turns ratio at the winding terminals of transformers, by definition, is

$$\frac{1}{n} = \frac{N_s}{N_p} = \frac{V_s}{V_p} = \frac{I_p}{I_s}$$

The CP and CA voltage and current transfer functions are

$$\text{CP } \frac{V_o}{V_g} = \frac{I_g}{I_o} = \frac{1}{n} \cdot D \; ; \; \text{CA } \frac{V_o}{V_g} = \frac{I_g}{I_o} = \frac{1}{n} \cdot \frac{1}{D'}$$

where D is the steady-state duty-ratio. Substituting for $1/n$ in the transfer functions for voltages and currents,

$$\text{CP}\quad \frac{V_o}{V_g}=\frac{V_s}{V_p}\cdot D=\frac{V_s}{V_g}\cdot D$$

$$\text{CP}\quad \frac{I_g}{I_o}=\frac{1}{n}\cdot D=\frac{I_p}{I_s}\cdot D=\frac{I_g}{I_s}\cdot D \Rightarrow \frac{V_o}{V_s}=\frac{I_s}{I_o}=D \Rightarrow V_s>V_o,\, I_s<I_o$$

$$\text{CA}\quad \frac{V_o}{V_g}=\frac{V_s}{V_p}\cdot\frac{1}{D'}=\frac{V_o}{V_p}\cdot\frac{1}{D'}$$

$$\text{CA}\quad \frac{I_g}{I_o}=\frac{1}{n}\cdot\frac{1}{D'}=\frac{I_p}{I_s}\cdot\frac{1}{D'}=\frac{I_p}{I_o}\cdot\frac{1}{D'} \Rightarrow \frac{V_p}{V_g}=\frac{I_g}{I_p}=\frac{1}{D'} \Rightarrow V_p>V_g,\, I_p<I_g$$

Fig. 2 (bottom) shows the Volksinverter push-pull primary-side CA (boost) configuration. In part 14 it was compared with a full-bridge CP circuit, highlighting design tradeoffs between primary-side push-pull and full-bridge switching. The push-pull (PP) drive of both of the Fig. 2 circuits provides more direct comparison between CP and CA based on equal transfer power and equal transformer core volume and window area, though their winding designs differ.

The CP must have a transformer with $1/n > 1$ that allows the CP circuit to output $V_o > V_g$. Because it is otherwise voltage-decreasing ($V_o/V_s < 1$), V_o is maximum at $D = 1$. In contrast, the CA circuit has ($V_p/V_g = V_s'/V_g > 1$) and unlimited V_o as $D \to 1$ and $1/D' \to \infty$. This frees $1/n$ to be optimized by other criteria.

The CP circuit must provide the minimum secondary voltage $V_s \geq V_o$ to sustain $V_o = 160$ V at a minimum $V_g = 20$ V (using Volksinverter design parameters); the CA circuit must supply the same V_o at maximum $V_g = 30$ V. Below $V_{g\min}$ the CP is unable to maintain inductor flux balance because $V_s < V_o$, and the CP secondary requires a higher $1/n$. Above $V_{g\max}$ the CA inductor has flux imbalance for $V_s' = n{\cdot}V_s = n{\cdot}V_o < V_g$. The CP and CA $1/n$ ratio is found by solving for $1/n$;

$$\text{CP}\ \frac{1}{n}=\frac{V_o/D}{V_{g\min}};\ \text{CA}\ \frac{1}{n}=\frac{D'\cdot V_o}{V_{g\max}}$$

Their ratio is

$$\frac{\frac{1}{n}(\text{CP})}{\frac{1}{n}(\text{CA})}=\frac{V_{g\max}}{V_{g\min}}\cdot\frac{V_o/D_{CP}}{V_o\cdot D_{CA}'}=\frac{V_{g\max}}{V_{g\min}}\cdot\frac{1}{D_{CP}\cdot D_{CA}'}$$

The CP secondary winding has higher voltage and lower current, or more turns of smaller wire. The transfer power at constant V_o is greatest when output current I_o is made as large as possible. CP conversion of inductor and passive switch follows the secondary winding. It converts secondary current to a higher value of $I_o = I_s/D > I_s$. This conversion negates the secondary-winding turns disadvantage of lower current.

The CA requires a lower $1/n$; the primary winding has higher voltage and lower current—more turns of smaller wire size with lower current at a higher voltage of V_s', whereas the CP primary winding must conduct the full I_g. Primary-side CA switches and windings benefit from a higher resistance circuit—higher voltage ($V_p = V_s' > V_g$) and lower current ($I_p < I_g$). Because CA $I_p < I_g$, to maximize $I_s = I_p/(1/n)$ the CA has lower $1/n$; it has fewer secondary turns of larger wire than the CP transformer.

The CA and CP configurations show no advantage in power transfer over each other. The transformer winding area required to transfer the same power is not dependent on V_p/I_p or V_s/I_s because smaller wire for less current requires more turns for higher voltage. The same winding area is filled with wire though of a different size and turns.

Relative Merits Of CA And CP Circuits

The current form factors of active (MOSFET) and passive (diode) switches and their windings in series are performance factors for power-circuit design. Their product combines them into the single parameter $\kappa_{QD} = \kappa_Q \cdot \kappa_D$. Resistive loss in switches and windings is lowest when $\kappa_{QD} = 1$, its minimum value. The plots of κ_{QD} are graphed in Fig. 3; the CP-PP plot is labeled $\kappa_{QDCP}(D)$ with D and the CA-PP plot is $\kappa_{QDCA}(D')$ with D' on the horizontal axis.

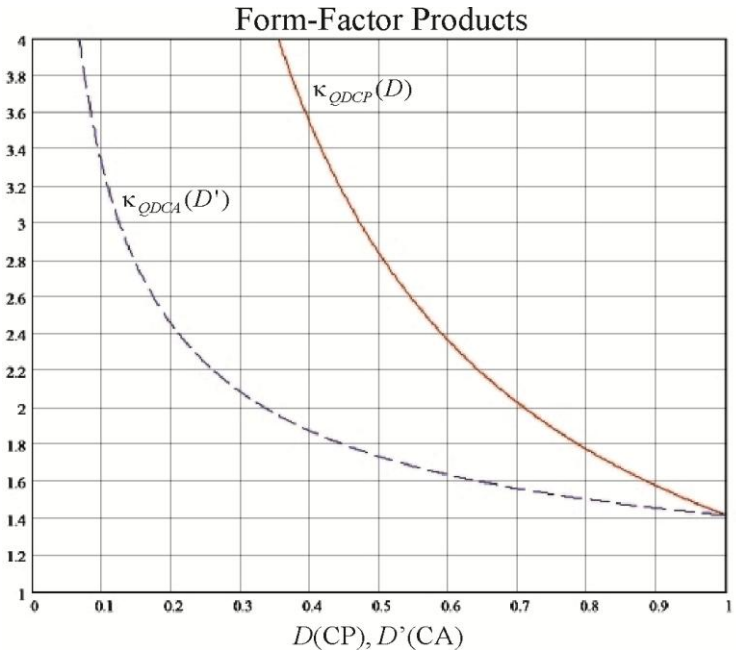

Fig. 3. Winding-loss and switch-loss performance plots of form-factor products $\kappa_{QDCP}(D)$ for the CP-PP (solid, red) and $\kappa_{QDCA}(D')$ for the CA-PP (dash, blue).

The form-factor products in D and D' are

$$\kappa_{QDCP}(D) = \frac{\sqrt{2}}{D} \;;\; \kappa_{QDCA}(D') = \sqrt{\frac{1+D'}{D'}}$$

They are both minimal at extremes of D. The optimal CA-PP duty-ratio, as derived in part 11[26], is based on equating $\kappa_Q = \kappa_D$. This constraint sets $D_{CA}' = 0.618$ ($D_{CA} = 0.382$) where the current form factor product $\kappa_{QDCA} \approx 1.618$. CP κ_Q and κ_D do not intersect; $\kappa_Q > \kappa_D$.

Furthermore, a CP operating-point for nominal D is set and variation of duty-ratio around it allows for converter control. The optimal $D_{CP} = 1$, but that leaves no control range on the high side, and the D_{CP} operating-point must be made less than 1.

A maximum range value of $D_{CP} = 0.925$ is not unreasonable because at this high value of D, switching times are reduced to $(0.0375) \cdot T_s$. At 75 kHz, $T_s = 13.33$ µs, and switching times (on and off) are 500 ns each. Although newer gate drivers can switch faster than this, design tolerance that includes delay in control circuits such as

the peak-current comparator make 0.5 µs typical. A CP D = 0.809 provides a wider operating range to avoid the degenerate case of D = 1.

From Fig. 3 it is evident that the CA-PP has lower κ_{QD} than the CP-PP circuit over the full range of D < 1. At CP D = 0.925 and CA D' = 0.618, $\kappa_{QDCA}/\kappa_{QDCP}$ = 1.618/1.529 = 1.058, the CA has about 6% greater switch loss than the CP at their differing operating-points of D. For CP D = 0.809, $\kappa_{QDCA}/\kappa_{QDCP}$ = 1.618/1.748 = 0.926; the CA has about 7% less switch loss than the CP. Conclusion: CA and CP switch losses are comparable. Neither has a significant advantage over the other.

This analysis expands to include input voltage range. Both CP and CA inputs must operate between $V_{g\min}$ and $V_{g\max}$. Applying the Volksinverter numbers, the 1/n ratio of CP to CA is

$$\frac{\frac{1}{n}(\text{CP})}{\frac{1}{n}(\text{CA})} = \frac{V_{g\,\max}}{V_{g\,\min}} \cdot \frac{1}{D_{CP} \cdot D_{CA}'} = \frac{30\text{ V}}{20\text{ V}} \cdot \frac{1}{(0.809)\cdot(0.618)} = (1.5)\cdot(2) = 3$$

The CP requires 1/n to be 2 times larger (second factor) than for the CA at fixed port voltages based on operating-point, and when the V_g range is included, it is 3 times larger. The ranges of D(CP) and D'(CA) are given in the table. The CP operating-point is extended to its practical maximum of D = 0.925.

Table. Ranges of CP-PP and CA-PP over V_g range.

V_g, V	V_o/V_g	D(CP)	D'(CA)
20	8.0	0.925	0.50
25	6.4	0.740	0.625
30	5.33	0.617	0.75

From the table, the range of D around midrange is ΔD(CP) = ±15.4% and ΔD(CA) = $\Delta D'$(CA) = ±12.5%. The CP ΔD is about 23% greater than for the CA. The CA × 3 1/n of the CP at $V_{g\max}$ results in a larger V_s that requires a smaller value of D for a constant V_o. At the midrange operating-point of D(CP) = 0.74, $\kappa_{QDCP} \approx 1.91$. At D' = 0.618, where CA $\kappa_D = \kappa_Q$, $\kappa_{QDCA} \approx 1.618$, and reduction in power loss is about 15.3%. At the low end of D(CP) = 0.617 and $\kappa_{QDCP} \approx 2.29$, whereas D'(CA) = 0.50 and $\kappa_{QDCA} \approx 1.732$, or 24% less loss of the CA at the low end of the operating range. (The same advantage of lower loss accrued to the DBPP over the CP-BRG in part 14.)

Both transfer circuits in Fig. 2 have windings in series with switches that conduct the same currents. The Fig. 3 graph applies to both series switches and windings, and the CA circuit has over the entire range of D (or D') a lower κ_{QD}, hence both lower winding and switch losses.

The additional winding loss of the CP-PP affects transformer transfer-power density and requires a somewhat larger size of transformer. Its primary winding design is also made more difficult because its wire (or turn bundle) size is larger than for the CA, having fewer turns at higher current. The larger the wire relative to the allotted winding area, the more difficult it is to find a dimensional fit that fills the area with conductor for maximum winding utilization. As we saw in the CA converter transformer design (part 17), this is a major design constraint for low-R_g designs.

The larger 1/n of the CP, farther from n = 1/n = 1, has a greater difference in turns between windings. The extent of coupling depends on how the windings are configured, such as bifilar or sequential, interleaved or not. Windings with a large turns difference couple to the core to a differing extent, resulting in imbalance between leakage inductance L_l of the windings. (Both CA and CP circuits require snubbing to dissipate leakage energy and damp resonances with switch capacitance on both windings.)

Tripling the number of CP secondary turns results in more layers and more winding loss. Its reduced wire size allows more turns per layer, hence fewer layers, reducing eddy-current loss. For CP efficiency, $V_s - V_o$ is minimized by maximizing D (hence minimizing κ_{QD}), and this also minimizes I_o/I_s, reducing the difference in wire size between CP and CA secondary windings. Hence, $1/n >> 1$ is somewhat disadvantageous.

Magnetizing current i_m is the sloping ripple on otherwise square-wave current waveforms and contributes to core saturation and winding loss. It is related to primary-circuit flux $\lambda_p = V_p \cdot \Delta t = L_p \cdot i_{mp}$. CP on-time is transfer-time

$$\Delta t = \text{CP } D \cdot T_s > \text{CA } D' \cdot T_s$$

However, the CA has higher V_p, and flux is the voltage-time product. Thus

$$\text{CA } \lambda_p = V_p \cdot t_{off} = V_p \cdot (D' \cdot T_s) = (V_g / D') \cdot (D' \cdot T_s) = V_g \cdot T_s$$
$$\text{CP } \lambda_p = V_p \cdot t_{on} = V_g \cdot (D \cdot T_s) < V_g \cdot T_s$$

The λ_p values produce a CP advantage. It is small because CP $D \approx 1$. Primary magnetizing current $i_{mp} = \lambda_p / L_p$, and with fewer turns, CP L_p < CA L_p and thus CP i_{mp} > CA i_{mp}. Although CP inductance is less, so is flux, and by about the same fraction, giving neither CP or CA an advantage over the other; both have comparable magnetizing current ripple.

During off-time, CP i_m transfers to the secondary winding to become i_{ms}. It reduces rectifier inductor current and hence power loss for one branch of a FW rectifier but adds to the other branch. No advantage emerges for reduced i_{mp}.

Last but not least, the three-level current waveshape of the CA primary circuit is its distinguishing characteristic and requires a somewhat larger transformer to achieve design power. The design-power values for the CA transformer over the V_g range are larger than for the CP. However, because CP-PP losses are higher, it must also be made larger. The two opposing effects tend to cancel, leaving it a fine point as to which is actually superior. The transformer primary-side design-power ratios (that include V_g range) for Volksinverter specifications are

$$\text{CP-PP } \frac{\overline{P}_{pd}}{\overline{P}_g} = \sqrt{\frac{V_{g\max}}{V_{g\min}}} = 1.225 \text{ ; CA-PP } \frac{\overline{P}_{pd}}{\overline{P}_g} = \sqrt{\frac{1}{2} \cdot \frac{V_{g\max}}{V_{g\min}} \cdot \left(1 + \frac{V_s'}{V_{g\min}}\right)} = 1.50 \text{ , } V_s' = 40 \text{ V}$$

At minimum (no flux margin) $V_s' = V_{g\max} = 30$ V, the CA-PP design-power ratio is 1.37, still larger than for the CP-PP by about 12%. The design choice of $V_s' = 40$ V for flux-balance margin for the inductor increases design power of the CA-PP to be larger by 22.4%, a significant difference and comparable to the CP-PP loss difference.

Conclusions? The CA-PP has less winding and switch loss at high V_g but requires larger transformer size to achieve its design power. The CA-PP has a more complicated, multi-mode control scheme. The CP-PP has inverted merits plus a turns ratio of 3 times the CA-PP transformer, with the attendant difficulties in the magnetics design.

Closure

What can we conclude in carrying through this long 25-part article series featuring a design template for what at first seemed like a relatively straightforward power-electronics design problem? In retrospect, battery-input inverters are not a trivial exercise in design. What was unexpected were the many and varied side-trips for answering auxiliary design questions that arose along the way. Design questions and considerations lead to others and those to still others.

The inverter stage introduced some new concepts in how to protect it, yet the circuit topology does not differ much from mainstream designs. Nor does it need to; this circuit is simple and quite optimal for the two-stage inverter scheme.

The proposed CA-PP transfer circuit for the converter stage was the highlight of the Volksinverter design and withstood (though barely) its engineering comparison to the major contender—the CP-PP—while also considering the CP-BRG full-bridge buck and the differential boost push-pull (DBPP) of part 13. In the end, none of these four circuit alternatives has a great advantage over the others, each with its relative merits.

For particular design projects (including those that go beyond inverter design), the differences that were identified and design equations derived for quantitative comparison of performance parameters might be the biggest benefit of the article series and a reason to keep a copy of the whole series in your power-electronics file on your computer(s). (Please tell interested colleagues about the *How2Power Today* series and offer them a copy by "word of mouse".)

I would be interested in hearing from you as a reader about not only your overall impression of the series but how it might have subsequently benefitted you (or misled you) in a particular design project. The series is far wider in its applicability than just battery inverters. To give it concreteness, the series has been presented in the form of a *design template* for converters with power ports having low voltage and high current—design parameters that appear increasingly in point-of-load (POL), uninterruptable power supply (UPS), and other applications following the trend of decreasing output voltages and increasing currents.

And finally, with so much analysis in this series, I cannot guarantee that all of it is correct. Some of it—the magnetics design in particular—extrapolates at a frontier of power-magnetics research. If you find errors (such as I noted in reference [26]), let me know; I will appreciate the correction(s).

If any of this is consolidated in the future into paper book form wherein subsequent corrections or refinements are more difficult to make, any corrections of possibly major gaffes are especially important. Even so, I hope that those of you who have paid particular attention to this long design exercise will have acquired from it both formulas and insights that empower your design skills as an engineer.

References

1. "Designing An Open-Source Power Inverter (Part 1): Goals And Specifications" by Dennis Feucht, How2Power Today, May 2021.
2. "Designing An Open-Source Power Inverter (Part 2): Waveshape Selection" by Dennis Feucht, How2Power Today, September 2021.
3. "Designing An Open-Source Power Inverter (Part 3): Power-Transfer Circuit Options" by Dennis Feucht, How2Power Today, April 2022.
4. "Designing An Open-Source Power Inverter (Part 4): The Optimal Power-Line Waveshape" by Dennis Feucht, How2Power Today, May 2022.
5. "Designing An Open-Source Power Inverter (Part 5): Kilowatt Inverter Circuit Design" by Dennis Feucht, How2Power Today, July 2022.
6. "Designing An Open-Source Power Inverter (Part 6): Kilowatt Inverter Control Circuits" by Dennis Feucht, How2Power Today, August 2022.
7. "Designing An Open-Source Power Inverter (Part 7): Kilowatt Inverter Magnetics" by Dennis Feucht, How2Power Today, September 2022.
8. "Designing An Open-Source Power Inverter (Part 8): Converter Control Power Supply" by Dennis Feucht, How2Power Today, November 2022.
9. "Designing An Open-Source Power Inverter (Part 9): Magnetics For The Converter Control Power Supply" by Dennis Feucht, How2Power Today, December 2022.
10. "Designing An Open-Source Power Inverter (Part 10): Converter Protection Circuits" by Dennis Feucht, How2Power Today, February 2023.

11. "Designing An Open-Source Power Inverter (Part 11): Minimizing Switch Loss In Low-Input-Resistance Converters" by Dennis Feucht, How2Power Today, March 2023.
12. "Designing An Open-Source Power Inverter (Part 12): Sizing The Converter Magnetics" by Dennis Feucht, How2Power Today, May 2023.
13. "Designing An Open-Source Power Inverter (Part 13): The Differential Boost Push-Pull Power-Transfer Circuit" by Dennis Feucht, How2Power Today, June 2023.
14. "Designing An Open-Source Power Inverter (Part 14): Boost Push-Pull Or Buck Bridge?" by Dennis Feucht, How2Power Today, July 2023
15. "Designing An Open-Source Power Inverter (Part 15): Transformer Magnetic Design For the Battery Converter" by Dennis Feucht, How2Power Today, March 2024.
16. "Designing An Open-Source Power Inverter (Part 16): Transformer Winding Design For the Battery Converter—Efficiency Range And Winding Allotment" by Dennis Feucht, How2Power Today, April 2024.
17. "Designing An Open-Source Power Inverter (Part 17): Transformer Winding Design For the Battery Converter—Alternative Configurations" by Dennis Feucht, How2Power Today, May 2024.
18. "Designing An Open-Source Power Inverter (Part 18): Transformer Winding Design For The Battery Converter—Secondary Winding Design" by Dennis Feucht, How2Power Today, July 2024.
19. "Designing An Open-Source Power Inverter (Part 19): Controller Design For The Battery Converter" by Dennis Feucht, How2Power Today, September 2024.
20. "Designing An Open-Source Power Inverter (Part 20): Converter Inductor Magnetic Design" by Dennis Feucht, How2Power Today, October 2024.
21. "Designing An Open-Source Power Inverter (Part 21): Converter Inductor Winding Design" by Dennis Feucht, How2Power Today, November 2024.
22. "Designing An Open-Source Power Inverter (Part 22): Converter Regulator Dynamics" by Dennis Feucht, How2Power Today, December 2024.
23. "Designing An Open-Source Power Inverter (Part 23): Inverter Driver Design Refinement" by Dennis Feucht, How2Power Today, January 2025.
24. "Designing An Open-Source Power Inverter (Part 24): Inverter Output Filter Conundrum" by Dennis Feucht, How2Power Today, February 2025.
25. "How To Optimize Turns For Maximum Inductance With refere Saturation" by Dennis Feucht, How2Power Today, April 2019.
26. In part 11, above Fig. 3, the text should be corrected to read: "Then κ_{QD}(BPP) < κ_{QD}(PP). The BPP minimum κ_{QD} is the same as for the PP, but the BPP operates at lower κ_{QD} than the PP over the full range of D < 1."

About The Author

Dennis Feucht has been involved in power electronics for 40 years, designing motor-drives and power converters. He has an instrument background from Tektronix, where he designed test and measurement equipment and did research in Tek Labs. He has lately been working on projects in theoretical magnetics and power converter research.

For further reading on power supply control topics, see the How2Power Design Guide, locate the Design Area category and select "Control Methods".